

Article

## Entropies in Alloy Design for High-Entropy and Bulk Glassy Alloys

Akira Takeuchi <sup>1,\*</sup>, Kenji Amiya <sup>1</sup>, Takeshi Wada <sup>1</sup>, Kunio Yubuta <sup>1</sup>, Wei Zhang <sup>2</sup>  
and Akihiro Makino <sup>1</sup>

<sup>1</sup> Institute for Materials Research, Tohoku University, 2-1-1, Katahira, Aoba-ku, Sendai 980-8577, Japan; E-Mails: amiya.k@imr.tohoku.ac.jp (K.A.); wada-t@imr.tohoku.ac.jp (T.W.); yubuta@imr.tohoku.ac.jp (K.Y.); amakino@imr.tohoku.ac.jp (A.M.)

<sup>2</sup> School of Materials Science and Engineering, Dalian University of Technology, Dalian 116024, China; E-Mail: wzhang@dlut.edu.cn

\* Author to whom correspondence should be addressed; E-Mail: takeuchi@imr.tohoku.ac.jp; Tel.: +81-22-215-2383; Fax: +81-22-215-2714.

Received: 19 July 2013; in revised form: 10 September 2013 / Accepted: 10 September 2013 / Published: 12 September 2013

---

**Abstract:** High-entropy (H-E) alloys, bulk metallic glasses (BMGs) and high-entropy BMGs (HE-BMGs) were statistically analyzed with the help of a database of ternary amorphous alloys. Thermodynamic quantities corresponding to heat of mixing and atomic size differences were calculated as a function of composition of the multicomponent alloys. Actual calculations were performed for configurational entropy ( $S_{\text{config}}$ ) in defining the H-E alloys and mismatch entropy ( $S_{\sigma}$ ) normalized with Boltzmann constant ( $k_B$ ), together with mixing enthalpy ( $\Delta H_{\text{mix}}$ ) based on Miedema's empirical model and Delta parameter ( $\delta$ ) as a corresponding parameter to  $S_{\sigma}/k_B$ . The comparison between  $\Delta H_{\text{mix}} - \delta$  and  $\Delta H_{\text{mix}} - \sqrt{S_{\sigma}/k_B}$  diagrams for the ternary amorphous alloys revealed  $S_{\sigma}/k_B \sim (\delta/22)^2$ . The zones S, S' and B's where H-E alloys with disordered solid solutions, ordered alloys and BMGs are plotted in the  $\Delta H_{\text{mix}} - \delta$  diagram are correlated with the areas in the  $\Delta H_{\text{mix}} - S_{\sigma}/k_B$  diagram. The results provide mutual understandings among H-E alloys, BMGs and HE-BMGs.

**Keywords:** high-entropy alloy; bulk metallic glass; configurational entropy; mismatch entropy; atomic size difference; mixing enthalpy; alloy design

**PACS Codes:** 61.43.Dq, 81.05.Kf, 05.70.Ce, 05.70.-a

---

## 1. Introduction

This paper principally describes high-entropy (H-E) alloys [1] and bulk metallic glasses (BMGs) [2], together with relevant high-entropy bulk metallic glasses (HE-BMGs) [3–7] by focusing on entropy as well as enthalpy from thermodynamic quantities. The H-E alloys and BMGs are classified into the same alloy group in point that they are formed into a solid solution, although they have completely different crystallographic structures. Specifically, H-E alloys are formed into a simple crystalline structure of bcc, fcc or their mixture, whereas BMGs are into a glassy phase. One might think that the H-E alloys and BMGs have not been developed under the same alloy design because of their difference in structure. On the contrary, H-E alloys and BMGs have been developed by focusing on the common three factors [2] in their alloy designs: (1) the number of elements ( $N$ ), (2) difference in atomic size, and (3) mixing enthalpy ( $\Delta H_{\text{mix}}$ ). The first factor numerically defines the H-E alloys as equi-atomic or near equi-atomic multicomponent alloys with elements of five or more ( $N \geq 5$ ), whereas most of the BMGs are as  $N \geq 3$ , excepting for a couple of binary alloys, such as Cu-Zr [8,9] and Ni-Nb [10] BMGs. The second factor in H-E alloys is not limited by definition but broad enough to cover the second Inoue's rule for BMGs. On the other hand, the third factor for the H-E alloys is also not defined, and BMGs principally requires them to possess negative values of  $\Delta H_{\text{mix}}$  for the atomic pairs of the constituent elements. Thus, the first to third factors in the alloy design for H-E alloys and BMGs can be dealt with numerical and thermodynamic quantities to see their correlations and differences.

The H-E alloys and BMGs are also deeply involved in another thermodynamic quantity—entropy. Specifically, the H-E alloys are characterized by configurational entropy ( $S_{\text{config}}$ ). In reality, H-E alloys are named after the following aspects that  $S_{\text{config}}$  is maximized at the equi-atomic composition in a system and that equi-atomic alloys exhibit  $S_{\text{config}}/R = \ln N$  where  $R$  the gas constant. More precisely, the latter aspect is used for defining H-E alloys directly with thermodynamic formula,  $S_{\text{config}}/R \geq \ln 5$  ( $\sim 1.61$  [11]), according to the requirement  $N \geq 5$ . On the other hand, a mismatch entropy ( $S_{\sigma}$ ) can be used for BMGs for describing the difference in atomic size among the constituent elements, whereas an alternative parameter for  $S_{\sigma}$  for the H-E alloys is Delta parameter ( $\delta$ ) [12]. By utilizing thermodynamic and numerical quantities, such as  $\Delta H_{\text{mix}}$ ,  $S_{\text{config}}$  and  $\delta$ , the stabilities of crystalline H-E alloys with disordered solid solutions have been analyzed in such a set of formulae of  $\Delta S_{\text{config}}/R > 1.61$ ,  $\delta < 4.6$ , and  $-2.6856\delta - 2.54 < \Delta H_{\text{mix}}/\text{kJmol}^{-1} < -1.28\delta + 5.44$ , as reported by Zhang and Zhou [11]. These numerical applicability with thermodynamic and numerical quantities for forming H-E alloys are of great useful for alloy design of H-E alloys, together with the other precious analyses given by Ng *et al.* [13] for an  $\text{Al}_{0.5}\text{CoCrCuFeNi}$  H-E alloy for its thermo-mechanical treatments combined with thermodynamic calculations, and by Cunliffe *et al.* [14] for their discussions of forming-abilities of H-E alloys and amorphous phase for a  $(\text{TiZrNbCu})_{1-x}\text{Ni}_x$  system. Thus, the authors herewith focus on an important aspect that the H-E alloys and BMGs are sufficiently described by numerical and thermodynamic quantities in their alloy designs. Hence, one can utilise numerical and thermodynamic descriptions when developing more new H-E alloys and BMGs, leading to the drastic increase in the number of alloys found in two decades to date. Furthermore, increasing the number of alloys greatly contributes to data mining and resultant statistic analysis of H-E alloys and BMGs as well as HE-BMGs. This analysis indicates that one can distinguish H-E alloys, BMGs and HE-BMGs by paying attentions to the fundamental differences in characteristics between H-E alloys and BMGs. Here, the fundamental

differences include the following aspects that the H-E alloys are crystalline alloys whereas the BMGs are glassy alloys and that the atomic size difference among the constituent elements are small for the crystalline H-E alloys with disordered solid solutions and large for BMGs. These aspects lead to no intersections of their alloys in the  $\Delta H_{\text{mix}}-\delta$  diagram. Under these circumstances, the authors, however, expect that unprecedented new alloys may be found in the analyses of characterizing the H-E alloys and BMGs. They are new HE-BMGs or new H-E alloys with  $\Delta H_{\text{mix}}$  and  $\delta$  values which apart from the conventional ones in the  $\Delta H_{\text{mix}}-\delta$  diagram.

The purpose of the present paper is to clarify the features of H-E alloys, BMGs and HE-BMGs by focusing on entropies and other numerical and thermodynamic quantities with the help of statistical analysis for these alloys.

## 2. Calculation Methods

The effect of atomic size differences on the formation of BMGs was evaluated with mismatch entropy ( $S_\sigma$ ) by referring to a concept proposed by Mansoori *et al.* [15]. In the original literature [15], Mansoori *et al.* proposed an equation of state for the mixture of hard spheres based on an averaging process over the two results of the solution of the Percus–Yevik integral equation for the mixture of hard spheres. It should be noted that  $S_\sigma$  can be calculated as functions of atomic diameters ( $d_i$ ) of the  $i$ -th constituent element and a parameter ( $\zeta$ ) that relates to packing fraction  $\rho$  where  $\zeta = 1 / (1 - \rho)$ . The actual formulations used for calculating  $S_\sigma$  are shown in Equations (1) to (5) where  $k_B$  is the Boltzmann constant and dimensionless parameters  $y_i$ 's ( $i = 1$  to 3) have a relationship  $y_1 + y_2 + y_3 = 1$  [15]. The formulations in Equations (2) to (5) used in the present work and our early study [16] are different from those in the original literature [15]. In calculating, a system including hard spheres of atoms was considered under  $\rho = 0.64$  for dense random packing structure that includes amorphous alloys, metallic glasses and BMGs. The details of the calculation were acquired from the original literature [15] where the mixing entropies consisting of four terms of ideal gas-, concentration-, packing- and misfit-term were taken into account. In the present study, only the misfit term  $S_\sigma$  was considered to describe the entropy of mixing concerning the differences in atomic radii. The values of  $d_i$ 's were acquired from literature [17].

$$S_{\text{config.}} / k_B = \left\{ \frac{3}{2}(\zeta - 1)y_1 + \frac{3}{2}(\zeta - 1)^2 y_2 - \left[ \frac{1}{2}(\zeta - 1)(\zeta - 3) + \ln \zeta \right] (1 - y_3) \right\} \quad (1)$$

$$y_1 = \frac{1}{\sigma^3} \sum_{j>i=1}^N (d_i + d_j)(d_i - d_j)^2 c_i c_j \quad (2)$$

$$y_2 = \frac{\sigma^2}{(\sigma^3)^2} \sum_{j>i=1}^N d_i d_j (d_i - d_j)^2 c_i c_j \quad (3)$$

$$y_3 = \frac{(\sigma^2)^3}{(\sigma^3)^2} \quad (4)$$

$$\sigma^k = \sum_{i=1}^N c_i d_i^k \quad (5)$$

Besides, configuration entropy ( $S_{\text{config.}}$ ) and mismatch entropy were also calculated in the present study. The  $S_{\text{config.}}$  was calculated on the basis of the fundamental knowledge on thermodynamics for counting the number of cases to distribute the solute and solvent atoms in a hypothetical lattice. Specifically,  $S_{\text{config.}}$  is given by Equation (6), with a gas constant ( $R$ ) and a fraction of the  $i$ -th elements in the alloy with  $N$  elements. The equi-atomicity principle of the H-E alloys makes it possible to describe the increase in  $S_{\text{config.}}$  with increasing  $N$ , as shown in Equation (7) [1].

$$S_{\text{config.}} / R = - \sum_{i=1}^N c_i \ln c_i \quad (6)$$

$$S_{\text{config.}} / R = \ln N \quad (7)$$

On the other hand,  $\Delta H_{\text{mix}}$  was computed based on Miedema's empirical method [18] using Equation (8). Equation 8 exhibits the parabolic nature of  $\Delta H_{\text{mix}}$  as a function of  $c_i$ , which is an approximated description for  $\Delta H_{\text{mix}}$  given in the original literature [18] in order to calculate  $\Delta H_{\text{mix}}$  simply and comprehensively. The  $\delta$  was calculated based on Equation (9) using the average atomic radius from that of the constituent elements shown in Equation (10) [12].

$$\Delta H_{\text{mix}} = 4 \sum_{j \neq i}^N \sum_{i=1}^N \Delta H_{ij} c_i c_j \quad (8)$$

$$\delta = \sqrt{\sum_{i=1}^N c_i \left(1 - \frac{r_i}{\bar{r}}\right)^2} \times 100 \quad (9)$$

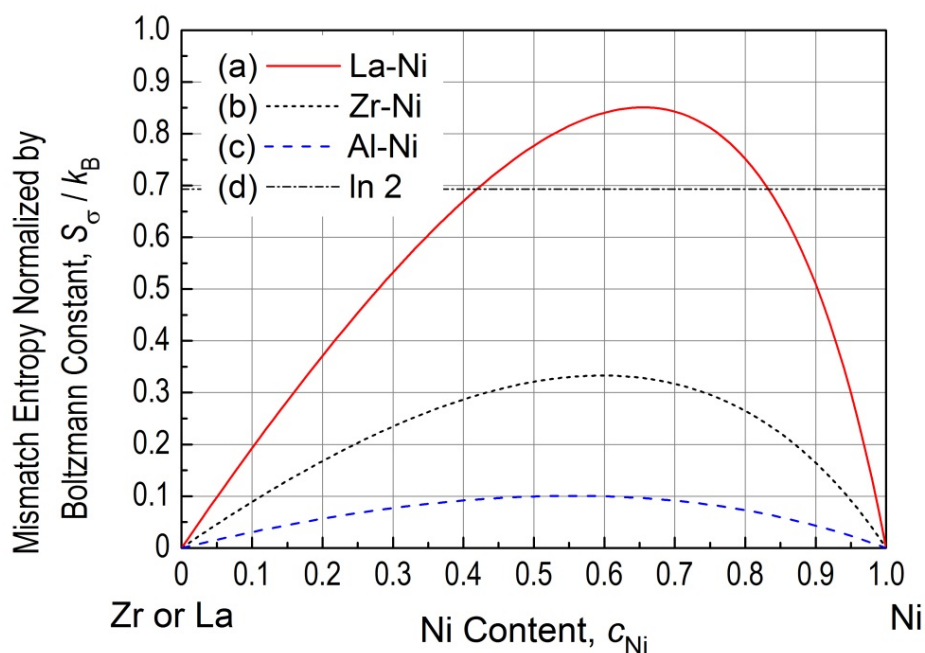
$$\bar{r} = \sum_{i=1}^N c_i r_i \quad (10)$$

### 3. Results and Discussion

First, the effect of atomic size differences on the formation of BMGs was evaluated with  $S_{\sigma}/k_B$  for Zr-Al-Ni and La-Al-Ni alloys where the atomic radius ( $r_i$ ) of La, Zr, Al and Ni were acquired from literature [17]:  $r_{\text{La}} = 0.182$  nm,  $r_{\text{Zr}} = 0.162$  nm,  $r_{\text{Al}} = 0.143$  nm and  $r_{\text{Ni}} = 0.125$  nm. One can expect that Zr-Ni and La-Ni sub-binary systems exhibit the greatest difference in atomic radius in Zr-Al-Ni and La-Al-Ni systems, respectively, according to these  $r_i$ 's. Figure 1 demonstrates the changes in  $S_{\sigma}/k_B$  for (a) La-Ni, (b) Zr-Ni and (c) Al-Ni systems as a function of Ni content, together with (d) a line of  $\ln 2$  for comparison. All the three curves (a–c) show asymmetry against the equi-atomic composition ( $c_{\text{Ni}} = 0.5$ ), indicating that the effect of a case for smaller atoms embedded in an atomistic environment of larger atoms are not the same to that of the opposite case. The three curves exhibit the maximum values at  $(c_{\text{Ni}}, S_{\sigma}/k_B) = (0.65, 0.851)$  for La-Ni,  $(0.60, 0.333)$  for Zr-Ni and  $(0.55, 0.101)$  for Al-Ni systems, indicating that atomic size effect is greater when the larger atoms of La, Zr or Al are solved as solution atoms in a Ni matrix with smaller atomic radius as a major atom. A possible explanation for this can be given when considering the opposite case of Ni as a minor and La, Zr or Al as major: The Ni atom will be placed at a interstitial site of the larger atoms, reducing the randomness of atomic arrangements of larger atoms in a system. Here, it should be noted that La-Ni system exhibits  $S_{\sigma}/k_B$  values larger than  $\ln 2$

at  $c_{\text{Ni}}$  ranging 0.42 to 0.82. The value of  $\ln 2$  is drawn in (d) with the broken dot line, and corresponds to  $S_{\text{config.}}/k_B$  at the equi-atomic composition for a binary alloy according to Equation (7) for  $N = 2$ . Thus, it should be noted that the La-Ni alloy near  $c_{\text{Ni}} \sim 0.5$  possesses considerably as large  $S_{\sigma}/k_B$  as the order of  $S_{\text{config.}}/k_B$  resulting from the atomic size differences only. This is an important aspect for BMG systems with appropriate large atomic size differences. The effect of atomic size difference is also important for the H-E alloy, but this effect can be ignored, since H-E alloys usually possess smaller atomic size differences than BMGs. In reality, some of the H-E alloys contains Ni and Al, but the maximum values is obtained at  $(c_{\text{Ni}}, S_{\sigma}/k_B)$  (0.55, 0.101), which is approximately 15% of  $\ln 2$ . Thus, Figure 1 suggests that both  $S_{\sigma}/k_B$  and  $S_{\text{config.}}/k_B$  contributes for the formation of BMGs, whereas  $S_{\text{config.}}/k_B$  contributes greatly than  $S_{\sigma}/k_B$  for H-E alloys. The limited contribution of  $S_{\sigma}/k_B$  for H-E alloys with disordered solid solutions could be explained by the Hume-Rothery rules [19] for forming solid solutions, which restrict the allowable maximum atomic size difference between solvent and solute elements in a solid solution. Specific explanations for stabilizing H-E alloys and destabilizing intermetallic compounds were given by Li *et al.* [20], that  $S_{\text{config.}} \sim 1.61R$  is almost the same magnitude to the melting entropy of most intermetallic compounds (about  $R-2R$ ) and by Hu *et al.* [21], that incorporation of Y element to an AlCoCrCuNiTi alloy resulted in forming intermetallic compounds due to the high chemical activity of Y element. Furthermore, it should be noted that competition between  $S_{\sigma}/k_B$  and  $S_{\text{config.}}/k_B$  can also make the composition of the mostly-stable solid solution deviate from absolute equi-atomic composition that maximizes  $S_{\text{config.}}/k_B$ . This competition sometimes results in that the optimization of compositions is required for H-E alloys from complete equi-atomic compositions.

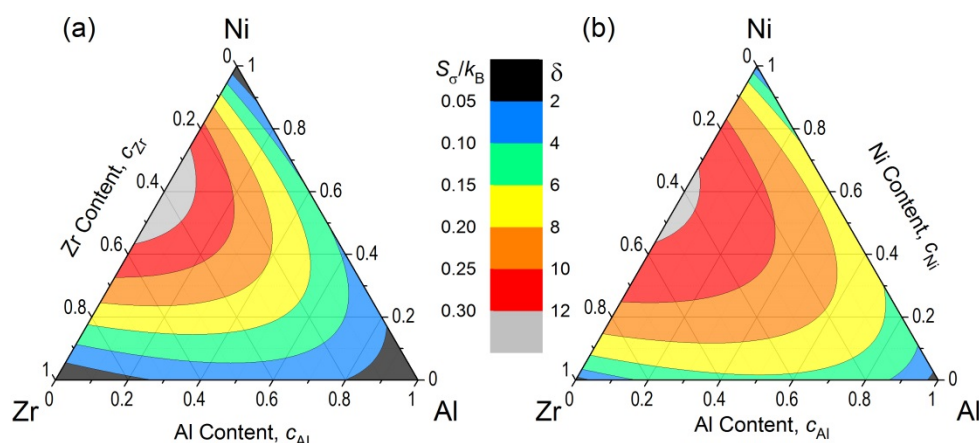
**Figure 1.** Mismatch entropy normalized by Boltzmann constant ( $S_{\sigma}/k_B$ ) for La-Ni, Zr-Ni and Al-Ni binary systems. The broken-dot line exhibits  $S_{\sigma}/k_B = \ln 2$ , which corresponds to the value of  $S_{\text{config.}}/k_B$  at the equi-atomic composition for a binary alloy.



A peculiar feature of  $S_{\sigma}/k_B$  for multicomponent system with more than two elements is that the maximum value of the  $S_{\sigma}/k_B$ ,  $S_{\sigma}/k_B|_{\text{max}}$ , is habitually given in a sub-binary side with the maximum and minimum atomic radii in a composition diagram. In other words, the addition of any elements with

intermediate radii cannot exceed the  $S_{\sigma}/k_B|_{\max}$  in the sub-binary alloy comprising the elements with the largest and smallest atomic radii. Figure 2a shows the changes in  $S_{\sigma}/k_B$  plotted for Zr-Al-Ni systems. The maximum values of  $S_{\sigma}/k_B$  is seen on the Zr-Ni sub-binary side around  $c_{\text{Ni}} \sim 0.55$ , as is shown for Zr-Ni binary system in Figure 1. The addition of Al with an intermediate atomic radius between Zr and Ni tends to decrease the  $S_{\sigma}/k_B$  values along the Al corner. This tendency of  $S_{\sigma}/k_B$  is essentially similar in  $\delta$  as shown in Figure 2b. Figure 2 explains that  $S_{\sigma}/k_B$  and  $\delta$  essentially exhibit the same tendencies in a composition diagram.

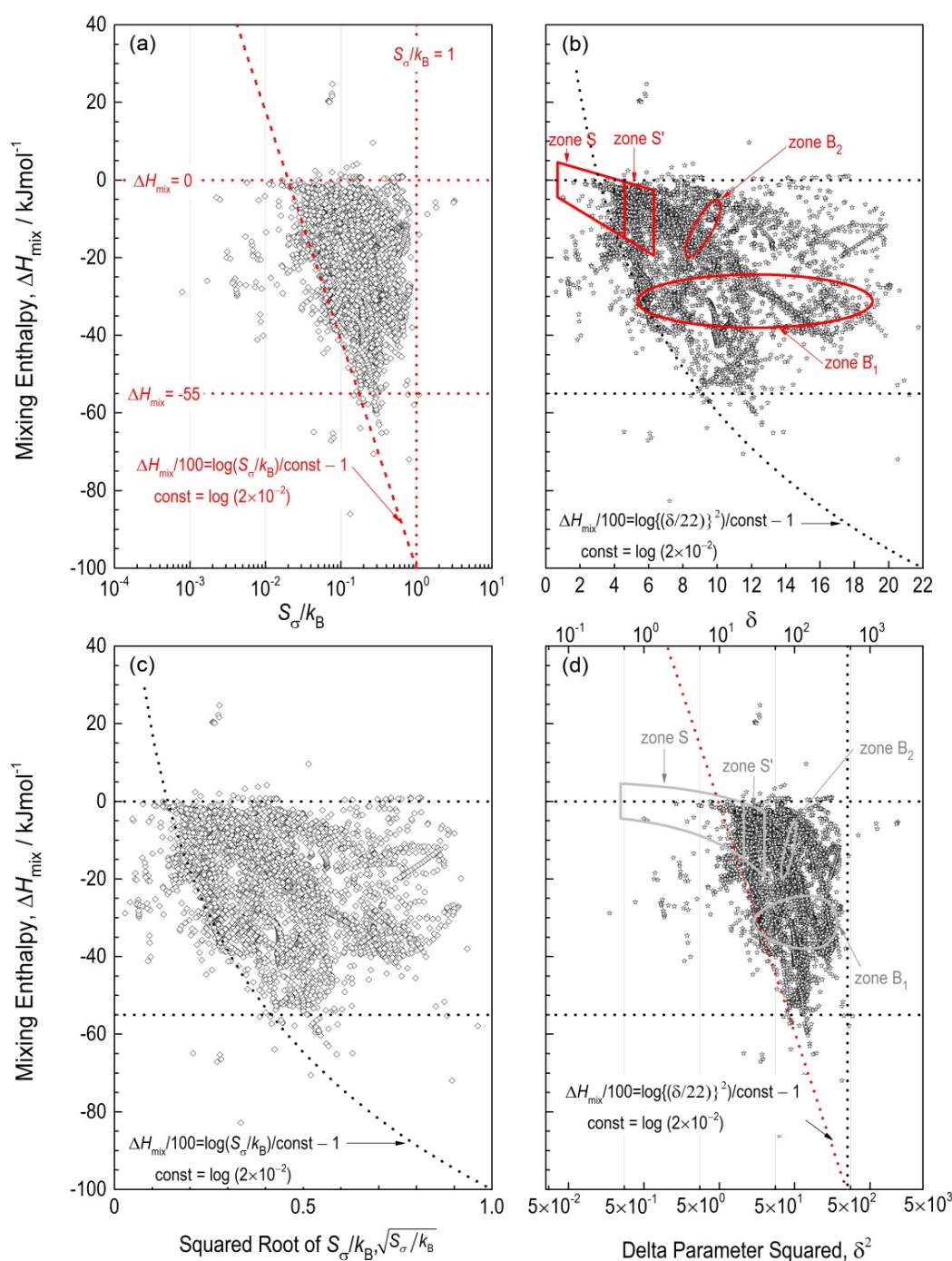
**Figure 2.** (a) Mismatch entropy normalized by Boltzmann constant ( $S_{\sigma}/k_B$ ) and (b) Delta parameter ( $\delta$ ) represented in contour lines in a composition diagram for Zr-Al-Ni system.



The  $\delta$  is frequently used in analyzing the features of H-E alloys, in particular, in a form of  $\Delta H_{\text{mix}}-\delta$  diagram [12]. The  $\Delta H_{\text{mix}}-\delta$  diagram has the same concept to  $\Delta H_{\text{mix}}-S_{\sigma}/k_B$  diagram [16], which was reported in the authors' early study to perform a statistical analysis of the effect of the second and third factor in alloy design for amorphous alloys including BMGs. These diagrams are similar in point that the values of  $\Delta H_{\text{mix}}$ ,  $\delta$  and  $S_{\sigma}/k_B$  were calculated as a function of composition where  $\Delta H_{\text{mix}}$  was calculated according to Equation (8). The calculation results of  $\Delta H_{\text{mix}}-S_{\sigma}/k_B$  and  $\Delta H_{\text{mix}}-\delta$  diagrams for the ternary amorphous alloys are shown in Figure 3, together with the plots of H-E alloys and BMGs. Here, it should be noted that x-axes in Figure 3a, d are in a logarithm scale for  $S_{\sigma}/k_B$  and  $\delta^2$ , respectively. Figure 3a, b are the original diagrams showing the relationships between  $\Delta H_{\text{mix}}-S_{\sigma}/k_B$  [16] and  $\Delta H_{\text{mix}}-\delta$ , [12] respectively. On the other hand, Figure 3c, d are other formulations of the diagrams for Figure 3a, b. Figure 3a, b show that no specific relationships are found between  $\log(S_{\sigma}/k_B)$  and  $\delta$ , since the plots of the amorphous alloys with the same data source [22] give different appearance in Figures 3a, b. In contrast, Figure 3(b,c) show clear similarities in plots of the ternary amorphous alloys. The plots in Figure 3b, c suggest that a relationship  $\sqrt{S_{\sigma}/k_B} \propto \delta$  (or  $S_{\sigma}/k_B \propto \delta^2$ ) holds for the ternary amorphous alloys. On the basis of this relationship, Figure 3 d with logarithm scale for x-axis ( $\delta^2$ ) is drawn by expecting that Figure 3(d) of the correspondence with Figure 3a. Here, it should be noted that x-axis ( $\delta^2$ ) in Figure 3d is intentionally set up in the range of  $5 \times 10^{-2}$  to  $5 \times 10^3$  for the correspondence between Figure 3a, d. Thus, it is shown that two sets of Figure 3a, d and Figure 3b, c are identical.



**Figure 3.** (a)  $\Delta H_{\text{mix}}-S_{\sigma}/k_B$  and (b)  $\Delta H_{\text{mix}}-\delta$  diagrams for the 6150 ternary amorphous alloys from 351 systems [22]. The trapezoid surrounded by broken lines in Figure 3a indicates the threshold values, in which ternary amorphous alloys are formed, whereas zones S, S', B's in Figure 3b exhibit the zones for H-E alloys with disordered solid solutions, H-E alloys with ordered solid solutions and BMGs, respectively, acquired from literature [12]. The solid and broken lines to in red to show the zones and areas demonstrate the original results, whereas black or gray ones are converted ones. Some of the data for Si-Ti-Zr ternary amorphous alloys in the original database [12] for Si and Ti contents were corrected according to the original reference [23], resulting in change in the plots in the original literature [16] in the areas of right triangle surrounded by broken line in Figure 3a. The x-axis ( $\delta^2$ ) in Figure 3d is intentionally set up in the range of  $5 \times 10^{-2}$  to  $5 \times 10^3$ .



The actual features of H-E alloys and BMGs are analyzed with the help of the plots of ternary amorphous alloys based on the two sets of diagrams mentioned above. Figure 3b shows that the density of the plots of the ternary amorphous alloys in zone S in  $\Delta H_{\text{mix}}-\delta$  diagram are less, in particular, at a part of the half to two-thirds from the left-side in zone S. This indicates that  $\Delta H_{\text{mix}}$  and  $\delta$  for most of the H-E alloys in zone S differ from those for the ternary amorphous alloys. On the other hand, zone S' for ordered alloys with ordered solid solutions are covered by the plots of the ternary amorphous alloys, indicating that the ordered alloys has the same trends with amorphous alloys. Besides, the half-down of the ellipse of zone B<sub>1</sub> almost matches the boundary of the plots in Figure 3b. These results for zones S, S', B<sub>1</sub> and B<sub>2</sub> were firstly clarified by computing  $\Delta H_{\text{mix}}$ ,  $\delta$  and  $S_{\sigma}/k_B$  simultaneously in the present study. Figure 3b revealed that the H-E alloys possess smaller atomic size difference than BMGs, which is shown in the fact that zone S is at the left side of zones B's. In addition, the H-E alloys have the smaller and negative  $\Delta H_{\text{mix}}$  than BMGs. The H-E alloys with disordered solid solutions are distinguished from ordered equi-atomic alloys by the boundary to separate zones S and S' at  $\delta = 4.6$ . The corresponding  $S_{\sigma}/k_B$  value would be  $\sqrt{S_{\sigma}/k_B} < 0.2$ , and thus,  $S_{\sigma}/k_B < 0.04$ , from Figure 3(c) according to the similarity in plots in Figure 3(b). The  $S_{\sigma}/k_B = 0.04$  is almost the half of the maximum of  $S_{\sigma}/k_B$  for Al-Ni system shown in Figure 1 and considerably smaller than  $\ln 2$ . Hence, the effect of atomic size for H-E alloys in zone S is thermodynamically negligible. However, this relatively-small difference in atomic size than that for BMGs is quite enough to restrict the atomic diffusion in H-E alloys, leading to excellent mechanical properties even at high temperatures [1]. In this sense, the H-E alloys possess an ideal atomic size differences to keep a simple single crystalline structure. The similarity in plots in Figure 3(b,c) suggests a relationship  $\sqrt{S_{\sigma}/k_B} \propto \delta$ , leading to a relationship in Equation (11),

$$\delta = 22\sqrt{S_{\sigma}/k_B}, \quad (11)$$

or  $\delta^2 = 484 \times (S_{\sigma}/k_B)$  from the statistical analysis shown in Figure 4. In Figure 4, the ternary amorphous alloys are plotted with open circles in Figure 4 to show the relationship between  $\sqrt{S_{\sigma}/k_B}$  and  $\delta$ , which is statistically approximated with linear formulae with and without intersection. As a result, the R-squared value ( $R^2$ ) was 0.99753 for the linear approximation with intersect drawn in broken line (a), whereas  $R^2 = 0.99753$  for the solid thick line (b) without intersection. The solid thin line (c) shows the relationship in Equation (1), indicating that the relationship between  $\sqrt{S_{\sigma}/k_B}$  and  $\delta$  for the ternary amorphous alloys can be approximated with Equation (11). The plots in Figure 4 exhibit good agreement with line (c) at  $\sqrt{S_{\sigma}/k_B} < 0.25$ , whereas they show larger deviations at  $0.25 < \sqrt{S_{\sigma}/k_B} \sim 1$ . Figure 4 suggests that Equation (11) holds for ternary amorphous alloys.

Further analysis was performed in detail by focusing on the relationships among H-E alloys, BMGs and H-E BMGs on the basis of  $\Delta H_{\text{mix}}-\delta$  and  $\Delta H_{\text{mix}}-\delta^2$  diagrams shown in Figure 5. Figure 5a is a revised  $\Delta H_{\text{mix}}-\delta$  diagram to the one reported in the authors' previous work [24] to which the sub x-axis according to Equation (11) and the data of 264 BMGs with the critical diameter ( $d_c$ ) ranging 0.2–12 mm [25] and 25 BMGs with  $d_c \geq$  half inch ( $\sim 12.3$  mm) [26] are added for comparison. Figure 5a indicates that almost all the BMGs and HE-BMGs are plotted under  $S_{\sigma}/k_B < 0.7 \sim \ln 2$ . The highest  $S_{\sigma}/k_B$ 's are seen in Zn-containing H-E BMGs [4,6], which are classified into Metal-Metal type



comprising metallic elements only. On the other hand, some of the BMGs in zone B<sub>1</sub> should contain Fe-TM-B (TM: transition metals) BMGs belonging to Metal-Metalloid type due to the inclusion of metalloid elements from B, C, Si, P and so forth. These BMGs belonging to Metal-Metalloid type also have high  $S_{\sigma}/k_B$ , because of the considerable difference in  $r_1$ 's between TM and B. Here, it should be noted that Al<sub>0.5</sub>TiZrPdCuNi H-E alloy with bcc single structure is separately plotted outside zone S [24]. The Al<sub>0.5</sub>TiZrPdCuNi H-E alloy was found in a procedure of finding H-E glassy alloy, and thus, the  $\Delta H_{\text{mix}}$  is larger and negative and  $\delta$  is larger than the conventional H-E alloys plotted in zone S. A reason for the Al<sub>0.5</sub>TiZrPdCuNi H-E alloy is found outside zone S had been unclear [24], but Figure 5(a) newly provides the following possible insights. The Al<sub>0.5</sub>TiZrPdCuNi H-E alloy is plotted at an area with gray solid ellipsoid where the ternary amorphous alloys are not plotted so densely as zone S' and plotted as less densely as zone S. Thus, it is expected that new H-E alloys may found when the alloys have  $-50 \leq \Delta H_{\text{mix}}/\text{kJmol}^{-1} \leq -40$  and  $8 \leq \delta \leq 10$  as well as  $6 \leq \delta \leq 8$  along the curve "Form. a" in Figure 3(a). This expectation to find out new H-E alloys with disordered solid solutions is only a necessary condition, but may open unprecedented new H-E alloys other than the area from zone S.

**Figure 4.** Relationship between  $\delta$  and  $(S_{\sigma}/k_B)^{0.5}$  for the 6150 ternary amorphous alloys from 351 systems [22]. The statistical analysis revealed the  $\delta \sim 22 \times (S_{\sigma}/k_B)^{0.5}$ .

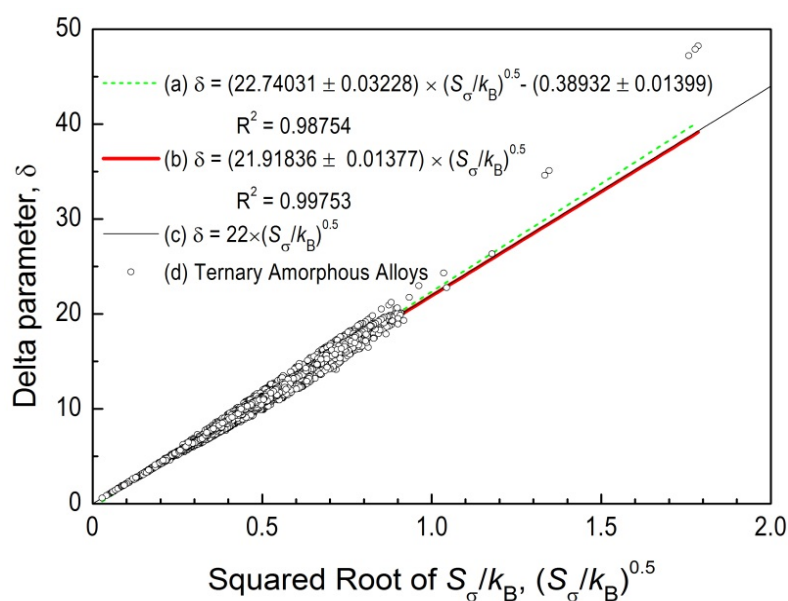
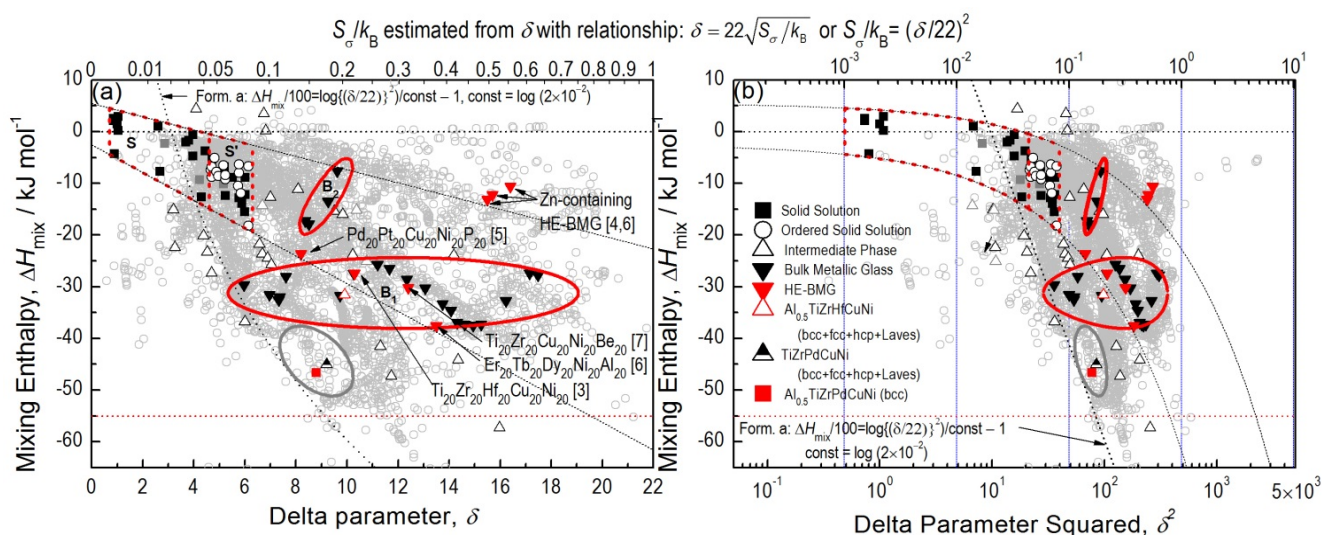


Figure 5 also provides other features of H-E alloys (zone S), ordered alloys (zone S'), BMGs (zones B<sub>1</sub> and B<sub>2</sub>) and HE-BMGs. For instance, zone B<sub>2</sub> for Cu- and Mg-based BMGs tends to be plotted inside the area between the upper- and lower lines extrapolated from zones S and S'. Specifically, the Cu- and Mg-conventional BMGs are plotted along two lines in Figure 5(a), in which a line is extrapolated from the upper-line of zones S and S' with a form of  $\Delta H_{\text{mix}} = -1.28 \delta + 5.44$  and another one is  $\Delta H_{\text{mix}} = -0.8 \delta + 3.5$ . Furthermore, HE-BMGs have a tendency to be plotted near the boundary of the extrapolated area. Furthermore, almost half of the BMGs in zone B<sub>1</sub> with higher  $\delta$  values trends to be in the extrapolated area. These tendencies suggest that BMGs in zone B<sub>2</sub> and those in right-half of zone B<sub>1</sub> and HE-BMGs can be categorized into the same group materials in point that their plots are within the lines extrapolated from zones S and S' in Figure 5. This can be a universal interpretation of

the H-E alloys, BMGs and HE-BMGs obtained from the statistical analysis. Hence, the results obtained in the present study to correlate  $S_\sigma$  with  $\delta$  as  $S_\sigma/k_B \sim (\delta/22)^2$  provides the mutual understandings among the H-E alloys, BMGs and HE-BMGs, and will be useful for further development of the alloys in near future. The authors have succeeded in correlating  $S_\sigma/k_B$  with  $\delta$ , where the former and latter are separately used for describing the atomic size differences for BMGs and H-E alloys, respectively. The authors anticipate that more new H-E alloys with disordered solid solutions, are found based on the results of the present study, as the  $\text{Al}_{0.5}\text{TiZrPdCuNi}$  H-E alloy found in a procedure of developing new H-E glassy alloy can be explained in the present study.

**Figure 5.** (a)  $\Delta H_{\text{mix}}-\delta$  and (b)  $\Delta H_{\text{mix}}-\delta^2$  diagrams, in which the data of H-E alloys, ordered alloys, intermetallic phases and BMGs including HE-BMGs. The  $S_\sigma/k_B$  is estimated from  $\delta$  with a relationship:  $S_\sigma/k_B = (\delta/22)^2$ .



#### 4. Conclusions

High-entropy (H-E) alloys, bulk metallic glasses (BMGs) and H-E BMGs (HE-BMGs) were analyzed for their configurational and mismatch entropies ( $S_{\text{config}}$  and  $S_\sigma$ ) as well as mixing enthalpy ( $\Delta H_{\text{mix}}$ ) and Delta parameter ( $\delta$ ). The analysis with the help of a database of ternary amorphous alloys revealed that a formula,  $S_\sigma/k_B \sim (\delta/22)^2$ , holds from the comparisons of the plots of the amorphous alloys in  $\Delta H_{\text{mix}}-S_\sigma/k_B$  and  $\Delta H_{\text{mix}}-\delta$  diagrams. The formula,  $S_\sigma/k_B \sim (\delta/22)^2$ , firstly correlates the  $S_\sigma/k_B$  for BMGs and  $\delta$  for H-E alloys, leading to the mutual understanding of the both alloys. It was found that the results can be used to explain the  $\text{Al}_{0.5}\text{TiZrPdCuNi}$  alloy is obtainable with different area to zone S for H-E alloys in  $\Delta H_{\text{mix}}-\delta$  diagram by focusing on the density of the plots of ternary amorphous alloys.

#### Acknowledgments

This work was supported by Grant-in-Aid for Scientific Research from Japan Society for the Promotion of Science (JSPS): Grant Program of Scientific Research (B) with program title of “Fabrication of High-Entropy Bulk Metallic Glasses based on Confusion Principle, Clarification of their Properties and their Application” (grant number 24360284).

## Conflicts of Interest

The authors declare no conflict of interest.

## References

1. Yeh, J.W. Recent progress in high-entropy alloys. *Ann. Chim., Sci. Mat.* **2006**, *31*, 633–648.
2. Inoue, A.; Takeuchi, A. Recent development and application products of bulk glassy alloys. *Acta Mater.* **2011**, *59*, 2243–2267.
3. Ma, L.Q.; Wang, L.M.; Zhang, T.; Inoue, A. Bulk glass formation of Ti-Zr-Hf-Cu-M (M = Fe, Co, Ni) alloys. *Mater. Trans.* **2002**, *43*, 277–280.
4. Gao, X.Q.; Zhao, K.; Ke, H.B.; Ding, D.W.; Wang, W.H.; Bai, H.Y. High mixing entropy bulk metallic glasses. *J. Non-Cryst. Solids* **2011**, *357*, 3557–3560.
5. Takeuchi, A.; Chen, N.; Wada, T.; Yokoyama, Y.; Kato, H.; Inoue, A.; Yeh, J.W. Pd<sub>20</sub>Pt<sub>20</sub>Cu<sub>20</sub>Ni<sub>20</sub>P<sub>20</sub> high-entropy alloy as a bulk metallic glass in the centimeter. *Intermetallics* **2011**, *19*, 1546–1554.
6. Zhao, K.; Xia, X.X.; Bai, H.Y.; Zhao, D.Q.; Wang, W.H. Room temperature homogeneous flow in a bulk metallic glass with low glass transition temperature. *Appl. Phys. Lett.* **2011**, *98*, 141913–141913.
7. Ding, H.Y.; Yao, K.F. High entropy Ti<sub>20</sub>Zr<sub>20</sub>Cu<sub>20</sub>Ni<sub>20</sub>Be<sub>20</sub> bulk metallic glass. *J. Non-Cryst. Solids* **2013**, *364*, 9–12.
8. Xu, D.H.; Lohwongwatana, B.; Duan, G.; Johnson, W.L.; Garland, C. Bulk metallic glass formation in binary Cu-rich alloy series—Cu<sub>100-x</sub>Zr<sub>x</sub> (x = 34, 36, 38.2, 40 at.%) and mechanical properties of bulk Cu<sub>64</sub>Zr<sub>36</sub> glass. *Acta Mater.* **2004**, *52*, 2621–2624.
9. Wang, D.; Li, Y.; Sun, B.B.; Sui, M.L.; Lu, K.; Ma, E. Bulk metallic glass formation in the binary Cu-Zr system. *Appl. Phys. Lett.* **2004**, *84*, 4029–4031.
10. Xia, L.; Li, W.H.; Fang, S.S.; Wei, B.C.; Dong, Y.D. Binary Ni-Nb bulk metallic glasses. *J. Appl. Phys.* **2006**, *99*, 026103.
11. Zhang, Y.; Zhou, Y., Solid solution formation criteria for high entropy alloys. *Mater. Sci. Forum* **2007**, *561*, 1337–1339.
12. Zhang, Y.; Zhou, Y.J.; Lin, J.P.; Chen, G.L.; Liaw, P.K. Solid-solution phase formation rules for multi-component alloys. *Adv. Eng. Mater.* **2008**, *10*, 534–538.
13. Ng, C.; Guo, S.; Luan, J.H.; Shi, S.Q.; Liu, C.T. Entropy-driven phase stability and slow diffusion kinetics in an Al<sub>0.5</sub>CoCrCuFeNi high entropy alloy. *Intermetallics* **2012**, *31*, 165–172.
14. Cunliffe, A.; Plummer, J.; Figueroa, I.; Todd, I. Glass formation in a high entropy alloy system by design. *Intermetallics* **2012**, *23*, 204–207.
15. Mansoori, G.A.; Carnahan, N.F.; Starling, K.E.; Leland, T.W. Equilibrium thermodynamic properties of mixture of hard spheres. *J. Chem. Phys.* **1971**, *54*, 1523–1525.
16. Takeuchi, A.; Inoue, A. Calculations of mixing enthalpy and mismatch entropy for ternary amorphous alloys. *Mater. Trans. JIM* **2000**, *41*, 1372–1378.
17. The Japan Institute of Metals. *Metal Databook*, 4th Ed.; Maruzen Co. Ltd.: Tokyo, Japan, 2004; p. 8.
18. De Boer, F.R.B.; R.; Mattens, W.C.M.; Miedema, A.R.; Nissen, A.K. *Cohesion in Metals: Transition Metal Alloys*; North Holland Physics Publishing, a division of Elsevier Science Publishers B.V.: Amsterdam, The Netherlands, 1988; p. 758.

19. Hume-Rothery, W.; Mabbott, G.W.; Evans, K.M.C. The freezing points, melting points, and solid solubility limits of the alloys of silver and copper with the elements of the B sub-groups. *Philos. Trans. R. Soc. Lond. A* **1934**, *233*, 1–97.
20. Li, C.; Li, J.C.; Zhao, M.; Jiang, Q. Effect of alloying elements on microstructure and properties of multiprincipal elements high-entropy alloys. *J. Alloy. Compd.* **2009**, *475*, 752–757.
21. Hu, Z.H.; Zhan, Y.Z.; Zhang, G.H.; She, J.; Li, C.H. Effect of rare earth Y addition on the microstructure and mechanical properties of high entropy AlCoCrCuNiTi alloys. *Mater. Design* **2010**, *31*, 1599–1602.
22. Kawazoe, Y.M., T.; Suzuki, K.; Inoue, A.; Tsai, A.-P.; J.-Z, Yu.; Aihara, T., Jr.; Nakanomo, T. *Phase Diagrams and Physical Properties of Nonequilibrium Alloys, Group III Condensed Matter*; Springer Berlin Heidelberg: Berlin/Heidelberg, Germany, 1997; p. 295.
23. Takeuchi, A.; Yavari, A.R.; Inoue, A. Golden Mean analysis of bulk metallic glasses with critical diameter over half-inch for their mole fractions of compositions. *Intermetallics* **2009**, *17*, 696–703.
24. Whang, S.H. Glass forming property of a Ti-Zr-Si system determined by temperature-composition map. *Scripta Metall. Mater.* **1984**, *18*, 309–312.
25. Takeuchi, A.; Wang, J.Q.; Chen, N.; Zhang, W.; Yokoyama, Y.; Yubuta, K.; Zhu, S.L. Al<sub>0.5</sub>TiZrPdCuNi High-Entropy (H-E) alloy developed through Ti<sub>20</sub>Zr<sub>20</sub>Pd<sub>20</sub>Cu<sub>20</sub>Ni<sub>20</sub> H-E glassy alloy comprising inter-transition metals. *Mater. Trans.* **2013**, *54*, 776–782.
26. Yuan, Z.Z.; Bao, S.L.; Lu, Y.; Zhang, D.P.; Yao, L. A new criterion for evaluating the glass-forming ability of bulk glass forming alloys. *J. Alloy. Compd.* **2008**, *459*, 251–260.